



Unusual hydroxyl effect on fulvene endoperoxide decompositions



Ihsan Erden^{a,*}, John Basada^a, Daniela Poli^a, Gabriel Cabrera^a, Fupei Xu^a, Scott Gronert^{b,*}

^aSan Francisco State University, Department of Chemistry and Biochemistry, 1600 Holloway Avenue, San Francisco, CA 94132, USA

^bDepartment of Chemistry, Virginia Commonwealth University, 1001 West Main Street, Richmond, VA 23284, USA

ARTICLE INFO

Article history:

Received 3 March 2016

Revised 4 April 2016

Accepted 7 April 2016

Available online 8 April 2016

Keywords:

Fulvenes

Endoperoxides

Allene oxides

Cyclopropanones

Oxy-allyl

ABSTRACT

The thermal decomposition of fulvene endoperoxides ordinarily proceeds via an allene oxide intermediate affording oxepin-2(3*H*)-one derivatives. We have now uncovered new, unusual pathways in these decompositions where the presence of a hydroxyl group on the alkyl or aryl attached to the fulvene exocyclic double bond has a profound effect on the fate of the reactive intermediates derived from the unstable endoperoxides. Computational work supports the proposed mechanistic pathways.

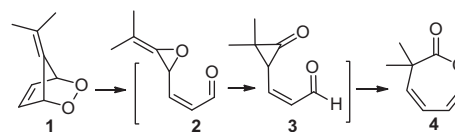
© 2016 Elsevier Ltd. All rights reserved.

Introduction

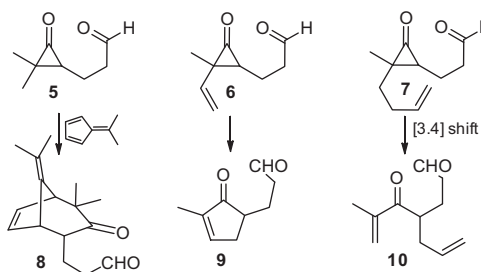
Fulvene-singlet oxygen (¹O₂) adducts are among the most strained and least stable bicyclic endoperoxides known to date.¹ It is not surprising that they are also the most intensely studied organic peroxides owing to the unusual pathways encountered during their decomposition. The most notable feature common to fulvene endoperoxides is the fact that the rupture of the labile O–O bond leads to reactive intermediates such as allene oxides and cyclopropanones (Scheme 1).^{2,3}

Though the latter had been implicated as likely precursors of the oxepin-3(2*H*)-ones (e.g., **4**) via electrocyclization of the transient cyclopropanone derivative, we have been able to verify the proposed mechanism by isolating a stable allene oxide from the photooxygenation of a saturated analog of **1** (*t*-butyl substitution at the exocyclic double bond).⁴ Moreover, we trapped the cyclopropanone intermediates derived from the saturated fulvene endoperoxides by Diels–Alder reactions,⁵ intramolecularly via vinylcyclopropanone–cyclopentenone cyclizations,⁶ and reported the first aliphatic examples of [3,4] sigmatropic shifts (Scheme 2).⁷

More recently we reported that endoperoxides derived from bicyclic fulvenes (i.e., 1,2-dihydropentalenes) undergo decomposition in an entirely different manner; the cyclopropanone intermediate in this case undergoes decarbonylation or intramolecular 1,3-acyl shift in a temperature-dependent reaction.⁸



Scheme 1. Normal course of fulvene endoperoxide isomerizations.



Scheme 2. Trapping experiments of cyclopropanones derived from saturated fulvene endoperoxides.

We now report that the course of the thermal isomerizations of fulvene endoperoxides is dramatically altered by incorporating a hydroxyl group into the substituents at the exocyclic double bond of the starting fulvene. The systems we studied, **11**, **12**, and **13**, are shown in Figure 1.

* Corresponding authors. Tel.: +1 415 338 1627; fax: +1 415 338 2384 (I.E.); tel.: +1 804 828 2753; fax: +1 804 828 8599 (S.G.).

E-mail addresses: ierden@sfsu.edu (I. Erden), sgronert@vcu.edu (S. Gronert).

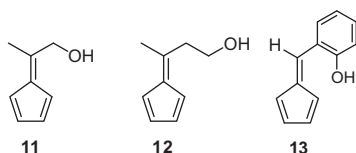
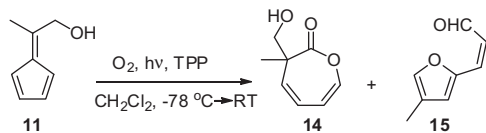
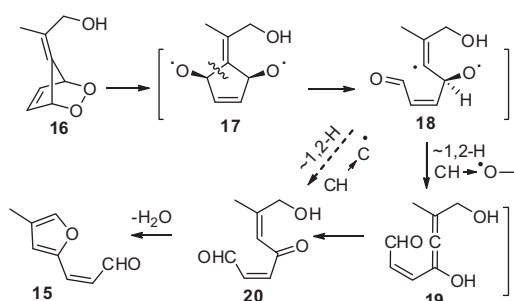


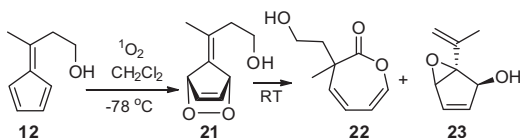
Figure 1. Fulvenes **11**, **12**, and **13** used in this study carrying OH groups.



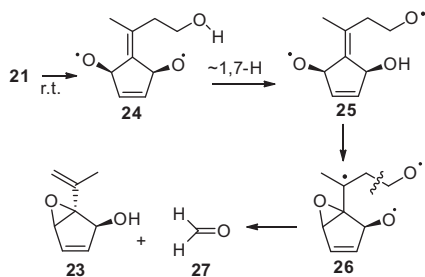
Scheme 3. Photooxygenation of **11** leading to **14** and **15**.



Scheme 4. Mechanism for furan **15** formation.



Scheme 5. Photooxygenation products from **12**.

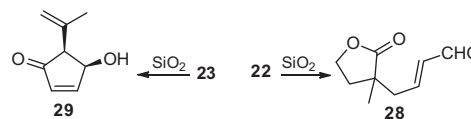


Scheme 6. Mechanism for the formation of **23** from **21**.

Results and discussion

All three substrates are readily available in high yields by the catalytic method we reported recently, or the stoichiometric method by Stone and Little.⁹

Photooxygenation of **11** in CH_2Cl_2 at -78°C , using TPP as sensitizer and allowing the photolysate to warm up to room temperature gave a mixture of two products, formed in a ratio of 3:1, respectively, which were separated from one another by flash chromatography and identified as **14** and **15** (combined yield 72%, Scheme 3).



Scheme 7. SiO_2 catalyzed isomerizations of **22** and **23**.

Whereas the formation of **14** was expected, furan **15** is an unusual product, and its formation is unprecedented. A favorable shift-often observed in oxygen centered radicals- is a 1,2-H shift to the oxygen radical¹⁰ (transition state enthalpy = -11.8 kcal/mol relative to **16**), giving an allenyl enol, **19**. Rapid tautomerization would also lead to **20**, and eventually to furan **15** via the corresponding γ -lactol followed by dehydration (Scheme 4).

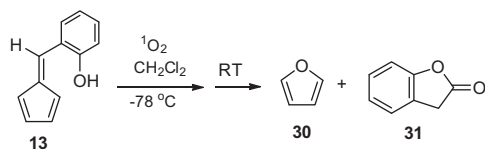
Alternatively, a 1,2-hydrogen atom transfer ($\text{HC}\rightarrow\text{C}$) in the oxygen-centered radical **18**, ensuing a common β -fission of the initial diradical might also account for the furan precursor (**18** \rightarrow **20** \rightarrow **15**), however, we consider a 1,2-H transfer to the adjacent vinyl highly unlikely due to a calculated activation enthalpy (M062x/6-311+G** with a PCM CH_2Cl_2 solvent model) that is 8.8 kcal/mol above the energy of **16**.¹¹

In the second system we studied (**12**) the hydroxyl group is one more carbon further down the alkyl chain than in **11**, and this subtle variation altered the course of the endoperoxide decomposition dramatically. Upon singlet oxygen addition at 78°C in CH_2Cl_2 , and subsequent warming the solution to room temperature, **12** gave a 2:1 mixture of **22**¹² and **23** in a combined yield of 68% (Scheme 5).

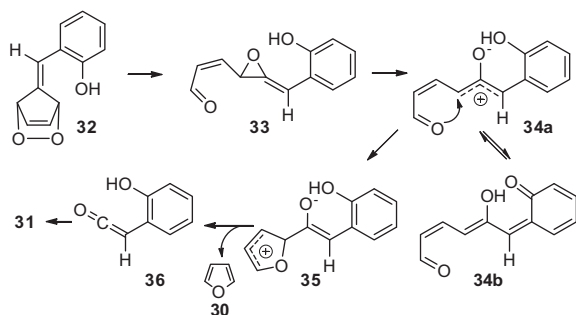
Again, the formation of the expected product **23** deserves no further comment. Compound **23**, on the other hand, apparently stems from a pathway wherein a fragmentation must have occurred since **23** lacks a CH_2O unit (formaldehyde) as compared to the endoperoxide **21** derived from **12**. A mechanism, consistent with the results is outlined in Scheme 6.

A reasonable pathway rationalizing the formation of **23** involves a rare 1,7-hydrogen atom transfer (HAT)¹³ from the hydroxyl group to the proximal oxygen-centered radical in **25**. Though rarely observed, it has been found that if the proper spatial orientation of the relevant hydrogen atom toward the oxygen- or carbon-centered radical is provided (an eight-membered transition state obviously suffers from a considerably unfavorable entropy of activation), 1,7-hydrogen abstractions can effectively compete with the more ubiquitous 1,5-H shifts. Molecular modeling at B3LYP/6-31C* level of theory indicates a favorable geometry for the 1,7-H abstraction with a H–O distance of 1.83 Å. The ensuing fragmentation in **26** leading to **23** and formaldehyde (**27**) is akin to the retro-Paterno–Buchi reaction, though carbon-centered 1,4-diradical intermediates have been implicated in the latter reactions.¹⁴ Although **22** and **23** could be separated from one another by flash chromatography, longer exposure of **23** to silica gel resulted in acid-catalyzed epoxide ring opening followed by a 1,2-hydride shift to give *cis*-4-hydroxyl-5-isopropenylcyclopent-2-enone (**29**). Moreover, compound **22** quantitatively isomerized to **28** during SiO_2 chromatography via acid-catalyzed trans-lactonization (Scheme 7).

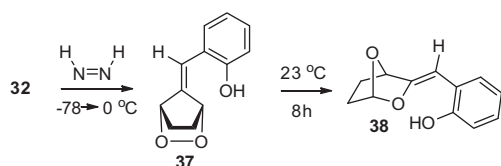
In the third system of our study, the hydroxyl group is placed in the *ortho* position of a phenyl group at C6 in the fulvene derived from salicyl aldehyde (**13**). Singlet oxygen addition was conducted under the same conditions as before at -78°C , however, CD_2Cl_2 was used as solvent in order to monitor the progress of the reaction by ^1H NMR and to avoid the loss of volatile products during the solvent removal by rotary evaporation. Indeed, upon warming the photolysate to room temperature, the ^1H NMR of the crude product mixture revealed that two products, furan (**30**) and 2-coumaranone (**31**, benzofuran-2(3*H*)-one) were formed in a 1:1 ratio (Scheme 8).



Scheme 8. Products **30** and **31** from the singlet oxygenation of **13**.



Scheme 9. Photooxidative fragmentation of fulvene **13** into furan (**30**) and 2-coumaranone (**31**).



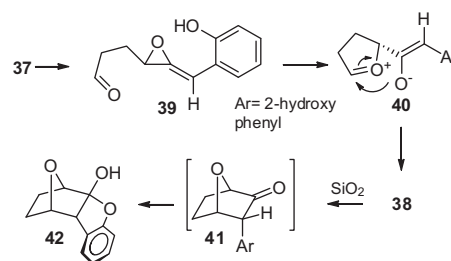
Scheme 10. Thermal isomerization of the saturated endoperoxide **37** to **38**.

The formation of **30** and **31** from the singlet oxygenation of **13** is remarkable in that the endoperoxide appears to have undergone a major fragmentation during one phase of decomposition. At first glance it is not obvious how the phenolic OH would affect the endoperoxide isomerization to the extent that two aromatic compounds, **30** and **31** would be split from one reactive intermediate. A plausible mechanism consistent with the experimental results is depicted in [Scheme 9](#).

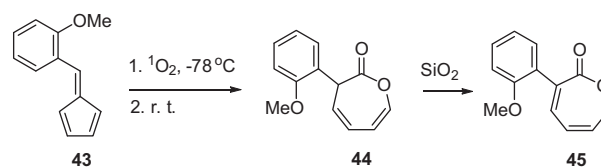
The key impact of the phenol is stabilization of the oxy-allyl intermediate, **34a**. Strong hydrogen bonding is possible with the phenolic OH and computational modeling (M062x/6-311+G** with a CH₂Cl₂ solvent model) suggests that it might be better described as a quinone methide, **34b**. In any case, the interaction provides over 20 kcal/mol of stabilization of the oxy-allyl intermediate relative to the allene oxide, **33**.

This creates a situation where the oxy-allyl intermediate is more stable than the allene oxide and cyclopropanone isomers by 18.5 and 9.3 kcal/mol, respectively, predisposing the system to follow the path in [Scheme 9](#) (ring-expansion to the lactone must pass through a cyclopropanone intermediate).¹⁵ In the absence of the hydroxyl substituent, the cyclopropanone is the preferred isomer on the potential energy surface by nearly 9 kcal/mol. In addition, the barrier to furan cyclization increases by 12 kcal/mol relative to the allene oxide ([Supplementary material, Table S1](#)).

Next, we studied the thermal behavior of the saturated analog of endoperoxide **32**. Selective diazene reduction of **32** at low temperature (−78 to 0 °C) gave the saturated endoperoxide **37**. An aliquot of the endoperoxide solution in CH₂Cl₂ was carefully concentrated under vacuum and a ¹H NMR spectrum was taken at 0 °C confirming the structure of **37**. It was left at room temperature overnight to decompose, and the crude product analyzed by



Scheme 11. Formation of **38** from allene oxide **39**; SiO₂ catalyzed isomerization of **38** to **42**.



Scheme 12. Photooxidative isomerization of **43** to the oxepinone derivatives.

¹H NMR. It showed the presence of one single product, the bicyclic acetal **38** ([Scheme 10](#)).

During the SiO₂ chromatography, **38** partially isomerized to the hemiacetal **42** by way of *endo*-3-(2-hydroxyphenyl)-7-oxabicyclo [2.2.1]heptan-2-one (**41**). The *endo*-stereochemistry in **42** was assigned based on the coupling constants (³J) of C1–H, C3–H and C4–H (³J_{3,4} = 6.0 Hz).¹⁶ This assignment is also consistent with the Z configuration we postulated for the allene oxide **33** derived from the unsaturated analog ([Scheme 11](#)).

Whereas the C–C cleavage in **35** leading to **36** and furan (**30**), an aromatic compound, is favored, this pathway is impeded in the saturated analog **39**. Intramolecular cyclization of **40** leads to the bicyclic acetal **38**. We previously reported similar intramolecular allene oxide–bicyclic acetal cyclizations during thermal isomerizations of saturated fulvene endoperoxides.^{4–6}

It is noteworthy that the hydroxyl group indeed alters the course of fulvene endoperoxide decompositions since the methoxy derivative of **13**, the fulvene derived from *o*-anisaldehyde (**43**)¹⁷ gave upon photooxygenation the expected oxepin-3(2*H*)-one **44** ([Scheme 12](#)). During chromatography on SiO₂ partial double bond isomerization to the conjugated oxepin-2(7*H*)-one isomer **45** occurred due to monosubstitution at C3.¹⁸

Conclusions

In conclusion, we report here some unusual pathways in fulvene endoperoxide decompositions brought on by the presence of substituents at C6 carrying hydroxyl groups: furan formation, 1,2- or 1,7-hydrogen shifts, and fragmentations represent significant deviations from the previously reported decomposition mechanisms observed in these reactions. Moreover, the proposed pathways have been supported by computational modeling in several cases.

Acknowledgments

I. Erden acknowledges financial support of this work by funds from the National Institutes of Health (Grant No. SC1 GM082340). D.P. is grateful to University of Florence, Italy, for financial support for a study visit at SFSU. The mass spectrometry work at SFSU was in part supported by a grant from the National Science Foundation (CHE-1228656) and is gratefully acknowledged.

S. Gronert acknowledges support from National Science Foundation (CHE-1300817). We also thank Dr. Robert Yen, SFSU, for the HRMS spectra and Mr. Krish Kumar for technical support.

Supplementary data

Supplementary data (experimental procedures and characterization data for all compounds; ^1H and ^{13}C NMR and FT-IR and HRMS data; full citation for Ref. 10; Table S1 contains calculated reaction enthalpies; and energies and geometries (xyz format) for all computed species.) associated with this article can be found, in the online version, at <http://dx.doi.org/10.1016/j.tetlet.2016.04.024>.

References and notes

1. Saito, I.; Matsuura, T. The Oxidation of Electron-Rich Aromatic Compounds. In *Singlet Oxygen*; Wasserman, H. H., Murray, R. W., Eds.; Organic Chemistry Series; Academic Press: New York, NY, 1979; Vol. 40, pp 511–574.
2. (a) Harada, N.; Suzuki, S.; Uda, H.; Ueno, H. *J. Am. Chem. Soc.* **1972**, *94*, 1777–1778; (b) Skorianetz, W.; Schulte-Elte, K. H.; Ohloff, G. *Angew. Chem., Int. Ed. Engl.* **1972**, *11*, 304–305; (c) Skorianetz, W.; Schulte-Elte, K. H.; Ohloff, G. *Helv. Chim. Acta* **1971**, *54*, 1913–1922; (d) Zhang, X.; Lin, F.; Foote, C. S. *J. Org. Chem.* **1995**, *60*, 1333–1338; (e) Erden, I.; Ocal, N.; Song, J.; Gleason, C.; Gärtner, C. *Tetrahedron* **2006**, *62*, 10676–10682.
3. Adam, W.; Erden, I. *Angew. Chem., Int. Ed. Engl.* **1978**, *17*, 210–211.
4. (a) Erden, I.; Drummond, J.; Alstad, R.; Xu, F. *Tetrahedron Lett.* **1993**, *34*, 1255–1258.
5. Erden, I.; Amputch, M. *Tetrahedron Lett.* **1987**, *28*, 3779–3782.
6. (a) Erden, I.; Drummond, J.; Alstad, R.; Xu, F. *J. Org. Chem.* **1993**, *58*, 3611–3612; (b) Erden, I.; Gärtner, C. *Tetrahedron Lett.* **2009**, *50*, 2381–2383.
7. Erden, I.; Xu, F.; Cao, W. *Angew. Chem., Int. Ed.* **1997**, *36*, 1516–1518.
8. Erden, I.; Ma, J.; Gärtner, C.; Azimi, S.; Gronert, S. *Tetrahedron* **2013**, *69*, 5044–5047.
9. (a) Coskun, N.; Erden, I. *Tetrahedron* **2011**, *67*, 8607–8614; (b) Erden, I.; Xu, F. P.; Sadoun, A.; Smith, W.; Sheff, G.; Ossun, M. *J. Org. Chem.* **1995**, *60*, 813–820; (c) Stone, K.; Little, R. D. *J. Org. Chem.* **1984**, *49*, 1849–1853.
10. Von Sontag, C. In *Free-Radical-Induced DNA Damage and its Repair: A Chemical Perspective*; Springer: Heidelberg, 2006; p 138.
11. Frisch, M. J. et al *Gaussian09, Revision C.01*; Gaussian: Wallingford CT, 2009. See Supplementary material for full reference.
12. Though compound **23** was identified in the crude ^1H NMR spectrum based on its characteristic signals, it was unstable on the silica gel column, in spite of pre-treatment with NEt_3 . It quantitatively underwent translactonization to **28** during chromatography (see Scheme 8).
13. To the best of our knowledge, a 1,7-H transfer from ROH to R'O' has not previously been reported. For a 1,7-H shift from a benzylic methylene to an alkoxy radical, see: Attouche, A.; Urban, D.; Beau, J.-M. *Angew. Chem., Int. Ed.* **2013**, *52*, 9572–9575. and references cited therein.
14. (a) Paterno, E.; Chieffi, G. *Gazz. Chim. Ital.* **1909**, *39*, 341; (b) Buchi, G.; Inman, C. G.; Lipinsky, E. S. *J. Am. Chem. Soc.* **1954**, *76*, 4327–4331.
15. Cyclopropanone formation is computed to be rate-limiting in the path to the ring-expanded lactone. The computed barrier to furan cyclization is 3 kcal/mol higher than the barrier to cyclopropanone formation. Although the polarized continuum model calculations are not able to reproduce the preference for the furan cyclization, they clearly highlight the dramatic impact of the phenol on the stability of the oxy-allyl intermediate and on the relative reaction barriers.
16. Numbering based on the uncyclized bicyclic ketone **41**.
17. Cini, M.; Bradshaw, T. D.; Woodward, S.; Lewis, W. *Angew. Chem., Int. Ed.* **2015**, *54*, 14179–14182.
18. See Supplementary material for experimental details and spectral characterization of **44** and **45**.